

Highly monodisperse supported metal nanoparticles by basic-ammonium functionalization of mesopore walls for industrially relevant catalysis

Jangkeun Cho,^{ab} Leilei Xu,^a Changbum Jo,^{*a} and Ryong Ryoo^{*ab}

^aCenter for Nanomaterials and Chemical Reactions, Institute for Basic Science (IBS), Daejeon 34141, Republic of Korea

^bDepartment of Chemistry, KAIST, Daejeon 34141, Republic of Korea

S1. Experiment

(1) Synthesis of $(\text{OEt})_3\text{-Si-C}_3\text{H}_6\text{-N}^+(\text{Me})_3(\text{OH})^-$

Trimethyl[3-(triethoxysilyl)-propyl]ammonium chloride ($(\text{OEt})_3\text{-Si-(CH}_2)_3\text{-N}^+(\text{Me})_3(\text{Cl})^-$, TCI) was dissolved in anhydrous ethanol (Merck). To replacing Cl^- with OH^- , anion-exchange resin (MTO-Dowex SBR LCNG OH form, Supelco) was added in the solution. After stirring for 5 h, the mixed solution was filtered to remove the resin part.

(2) Functionalization of mesoporous materials with $(\text{OEt})_3\text{-Si-C}_3\text{H}_6\text{-N}^+(\text{Me})_3(\text{OH})^-$

For typical organosilane-functionalization, 1 g of MFI silicate zeolite nanosponges (SZN) in a Pyrex[®] reactor was degassed at 300 °C for 4 h. After degassing, the Pyrex[®] reactor was placed in a glove box. We chose anhydrous ethanol as the solvent to achieve a good distribution of $-\text{C}_3\text{H}_6\text{-N}^+(\text{Me})_3(\text{OH})^-$ groups. It has been previously reported that hydrophilic ethanol could yield a homogeneous distribution of 3-aminopropylsilane groups on the pore walls of mesoporous silica.¹ Anhydrous ethanol (Merck) solution (15 mL) containing 2.0 mmol of $(\text{OEt})_3\text{-Si-(CH}_2)_3\text{-N}^+(\text{Me})_3(\text{OH})^-$ was poured to the degassed zeolite sample. The solution was heated to 60 °C for 12 h using ChemiStation, and cooled to room temperature. Then, the zeolite nanosponge was filtered from the solution and dried in a convection oven for 6 h. The ammonium group functionalized zeolite was denoted as AF-SZN.

For the functionalization of 1 g of MCM-48 and 1 g of $\gamma\text{-Al}_2\text{O}_3$, 2.0 mmol and 0.7 mmol of $(\text{OEt})_3\text{-Si-(CH}_2)_3\text{-N}^+(\text{Me})_3(\text{OH})^-$ were used, respectively. The rest of the functionalization process is the same as that used for the synthesis of the MFI zeolite nanosponge sample. The ammonium group functionalized MCM-48 and $\gamma\text{-Al}_2\text{O}_3$ were denoted as AF-MCM-48 and AF- $\gamma\text{-Al}_2\text{O}_3$, respectively.

(3) Synthesis of supported metal catalysts.

(3-1) Supported Ni catalysts by incipient wetness impregnation

For the preparation of 15-Ni-AF-SZN, 2.0 mL of 3.0 M aqueous solution of $\text{Ni}(\text{NO}_3)_2 \cdot 6\text{H}_2\text{O}$ was first titrated with 0.37 mL of 1.0 M NaOH solution ($\text{Ni}/\text{Na} = 20$, $\text{pH} \approx 5$) in a convection oven 60 °C. After taking out the solution from the oven, a part of clear solution (*i.e.*, 0.12 mL) was impregnated to 0.1 g of the dehydrated AF-SZN sample by incipient-wetness impregnation. After drying the sample at 100 °C, the dried samples were calcined at 350 °C for 4 h under an air stream (50 mL min^{-1}), followed by reduction at 400 °C for 4 h under H_2 flow (50 mL min^{-1}).

15-Ni-SZN and 15-Ni-AF-MCM-48 samples were synthesized according to the procedures described above; however, instead of the AF-SZN support, the SZN and AF-MCM-48 supports were used.

20-Ni-AF-SZN and 20-Ni-SZN samples were synthesized according to the procedures described above, but the concentration and added amounts of the Ni-nitrate solution used were different (5.0 M Ni solution and 0.11mL).

Similarly, 25-Ni-AF-SZN and 25-Ni-SZN samples were synthesized according to the procedures described above, but with different concentrations of Ni-nitrate solution (5.0 M Ni solution) and different added amounts (0.15 mL). In the case of the 30-Ni-AF-SZN, 7.0 M Ni-nitrate solution was used. In the titrated solution, 0.15 mL of the clear solution was impregnated to AF-SZN.

For the preparation of 15-Ni-AF- γ -Al₂O₃, 2.0 mL of 5.0 M aqueous solution of Ni(NO₃)₂·6H₂O was titrated with 0.61 mL of 1.0 M NaOH solution in a convection oven at 60 °C. After taking out the solution from the oven, a part of the clear solution (*i.e.*, 0.078 mL) was impregnated to 0.1 g of the dehydrated AF- γ -Al₂O₃ sample by incipient-wetness impregnation. The rest of the process is the same as that used for the preparation of 15-Ni-AF-SZN.

(3-2) Supported 15 wt% Ni catalysts by wet impregnation

In a typical synthesis, 4.0 mL of 0.075 M aqueous solution of Ni(NO₃)₂·6H₂O was titrated with 1.0 M of NaOH solution (Ni/Na = 16, pH ≈ 5). After putting 0.1 g of dehydrated support material in this solution, the mixture was stirred at room temperature for 12 h. The mixture was placed in a convection oven at 60°C under stirring until water was evaporated. After drying, the samples were calcined at 350 °C for 4 h under an air stream (50 mL min⁻¹), followed by reduction at 400 °C for 4 h under H₂ flow (50 mL min⁻¹). The resultant 15 wt% Ni supported catalysts exhibited a high dispersion of Ni nanoparticles, which are similar to the samples prepared by the incipient-wetness impregnation method.

(3-3) Supported SnO₂ catalysts by incipient wetness impregnation

Here, 2.1 mL of a 3.5 M NaOH aqueous solution was added dropwise to 2.0 mL of 3.0 M aqueous solution of SnCl₄·5H₂O (Sn/Na = 0.8, pH ≈ 1) at room temperature. Then, 0.15 ml of the clear solution was impregnated to 0.1 g degassed SZN and degassed AF-SZN samples. The resultant powder samples were dried at 100 °C for 12 h, and calcined at 350 °C for 4 h under an air stream (50 mL min⁻¹).

(3-4) Supported Cu catalysts by incipient wetness impregnation

To prepare 20 wt% Cu-supported catalysts, copper nitrate [Cu(NO₃)₂·3H₂O, Aldrich] was used as the precursor. Then, 2.0 mL of 3.4 M aqueous solution of Cu(NO₃)₂·3H₂O was titrated with 0.105 mL of 1.0 M Na₂CO₃ solution (Cu/Na = 32, pH ≈ 2) in an oven heated to 60 °C. In the titrated solution, only 0.12 mL of the clear solution was impregnated to SZN, MCM-48, AF-SZN, and AF-MCM-48 by incipient wetness impregnation method. After drying the sample at 100 °C, the dried samples were calcined at 350 °C for 4 h under an air stream (50 mL min⁻¹), and followed by reduction at 350 °C for 4 h under H₂ flow (50 mL min⁻¹).

For Cu supported γ -Al₂O₃, and AF- γ -Al₂O₃ catalysts, 2.0 mL of 5.5 M aqueous solution of Cu(NO₃)₂·3H₂O was titrated with 0.17 mL of 1.0 M Na₂CO₃ solution, and then, 0.078 mL of resultant clear solution was impregnated to dehydrated 0.1 g γ -Al₂O₃ and AF- γ -Al₂O₃. The rest of the process was identical to that used for the preparation of the 20-Cu-AF-SZN sample.

In the case of the Cu-CeO₂-supported catalyst, cerium nitrate [Ce(NO₃)₃·6H₂O, Aldrich] was sequentially impregnated onto the CuO-supported catalyst in an amount corresponding to Cu/CeO₂ = 2 (weight ratio). Subsequently, the powder sample was dried in a convection oven at 100 °C for 12 h. The dried sample was then calcined at 350 °C for 4 h under an air stream (50 mL min⁻¹), followed by reduction at 350 °C for 4 h under H₂ flow (50 mL min⁻¹). To prepare the Pt-CeO₂ supported catalyst, 1.0 mL of 0.05 M aqueous solution of Pt(NH₃)₄(NO₃)₂ was impregnated with AF-SZN. The powder sample was dried at 100 °C for 12 h, and calcined at 350 °C for 4 h under an air stream (50 mL min⁻¹). Then, cerium nitrate [Ce(NO₃)₃·6H₂O, Aldrich] was sequentially impregnated onto the PtO-supported catalyst in an amount corresponding to CeO₂/Pt = 10 (weight ratio). The rest of the procedure was same as that used for the synthesis of the Cu-CeO₂ supported catalyst.

S2. Characterization

The pH values of the titrated metal precursor solutions were measured using a Thermo Scientific™ Orion™ 3-Star Benchtop pH meter equipped with Orion 8157BNUMD Ross Ultra pH/ATC Triode. Powder X-ray diffraction (XRD) patterns were obtained at 2θ angles using a Rigaku Smartlab diffractometer equipped with Cu-K α radiation ($\lambda = 0.1541$ nm) at 40 kV and 30 mA. Scanning transmission electron microscopy (STEM) images were obtained with a Tecnai microscope operating at 300 kV (Titan G² ETEM). Before these measurements, the powder sample was suspended in acetone by ultrasonication. A few droplets of the suspended solution were placed on a Cu microgrid and dried under ambient conditions. N₂ adsorption-desorption isotherms were measured with a Micromeritics TriStar II volumetric adsorption analyzer at -196 °C. Prior to measurement, all samples were degassed under vacuum for 4 h at 300 °C, except for the ammonium-functionalized samples. To prevent organic decomposition, the ammonium-functionalized samples were degassed at 150 °C for 6 h. The specific surface area was calculated from the adsorption branch in the P/P₀ range of 0.05 to 0.2 using Brunauer-Emmett-Teller (BET) equations. The total pore volumes were derived from the amount of adsorption at a relative pressure close to 0.95. The solid ¹H magic angle spinning (MAS) NMR spectra were recorded using a Bruker Avance 400WB spectrometer at room temperature operated at 400 MHz for ¹H. The solid-state ¹H-NMR spectra were obtained under the following conditions: 3- μ s pulse width, 2-s relaxation delay, 10-kHz spinning rate, and 1,024 acquisitions. CO chemisorptions were measured with a Micromeritics ASAP 2020C with the pressure range of 25 to 500 Torr. Before CO chemisorption, the samples were heated up at a rate of 1 °C min⁻¹ to 400°C by using H₂ gas, followed by a 3 h hold at 400 °C. After evacuation at 400 °C for 1 h, the samples were cooled down to room temperature under He stream. Hydrogen chemisorption isotherms were obtained at room temperature using a lab-made volumetric adsorption apparatus. Before measurements, the Ni-loaded samples were heated up at a rate of 1 °C min⁻¹ to 400°C by using H₂ gas, followed by a 3 h hold at 400 °C. After evacuation at 400 °C for 2 h, the samples were cooled down to room temperature. The hydrogen chemisorption in H₂ uptake was determined by extrapolation of the adsorption isotherm to zero pressure.

S3. CO and H₂ chemisorption

The smaller the size of Ni nanoparticles, the greater the number of Ni atoms that could be exposed on the nanoparticle surfaces to perform catalytic functions. The fraction of the surface-exposed atoms among the total number of metal atoms is defined as the metal dispersion. In principle, if the stoichiometry between the surface atom and the adsorbate is known, the Ni dispersion can be determined by chemisorption. In this regards, we measured the CO and hydrogen chemisorption. The CO chemisorption data are shown in the table below. As the result shows, in the same series of AF-SZN zeolite with various Ni loadings (*i.e.*, 15, 20, and 25 wt%), the CO chemisorption proportionally increased with the Ni content. In contrast, in the case of 15, 20, and 25 wt% Ni loadings on SZN, similar CO chemisorption values (0.6 – 0.8 mmol g⁻¹) were obtained regardless of the metal loading. This result is consistent with the particle size trends depending on the metal content and the supporting material. However, the chemisorption data may not be over-interpreted to determine the metal dispersion, whereas CO chemisorption on supported nickel can overestimate the metal dispersion because of carbonyl formation, particularly when the CO contact time is long.^{2,3,4} Our hydrogen chemisorption data were also consistent with the aforementioned particle size trends, similar to the CO chemisorption. Hydrogen chemisorption is free from carbonyl formation, but it can still be complicated with unreduced Ni phases if Ni is not completely reduced.

Support	Ni content (wt%)	CO uptake (mmol g ⁻¹)	H ₂ uptake (mmol g ⁻¹)
AF-SZN	15	2.22	0.29
AF-SZN	20	2.78	0.36
AF-SZN	25	3.25	0.40
SZN	15	0.66	0.10
SZN	20	0.75	-
SZN	25	0.81	-
AF-MCM-48	15	2.02	0.28
AF- γ -Al ₂ O ₃	15	1.95	0.31

Table S1. BET surface area and pore volume for AF-SZN, 15-Ni-AF-SZN, 20-Ni-AF-SZN, and 25-Ni-AF-SZN.

Sample	BET surface area (m ² g ⁻¹) ^a	Pore volume (cm ³ g ⁻¹) ^a	BET surface area (m ² g ⁻¹) ^b	Mesopore volume (cm ³ g ⁻¹) ^b
AF-SZN	550	0.55	550	0.44
15-Ni-AF-SZN	372	0.37	437	0.33
20-Ni-AF-SZN	302	0.32	378	0.29
25-Ni-AF-SZN	254	0.28	339	0.26

^aBET surface area and pore volume were determined using the total weight of the sample.

^bBET surface area and pore volume were determined using only the weight of the zeolite sample. In that, we normalized the sample weight to only SZN by dividing 0.85, 0.80, and 0.75, respectively.

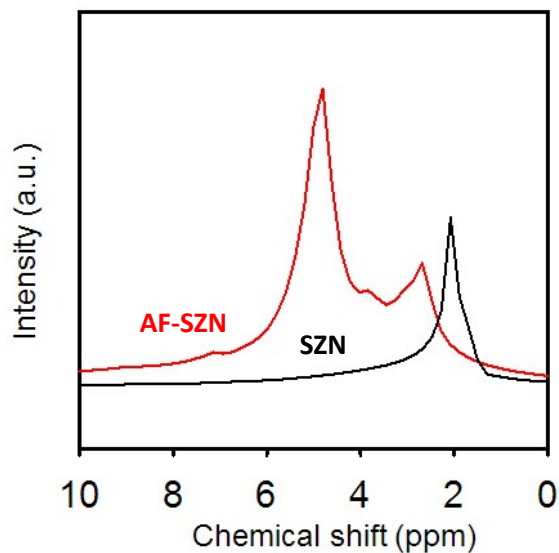


Fig. S1 Solid state ^1H -NMR spectrum of MFI zeolite nanosponge (SZN) and its functionalized form with $-\text{C}_3\text{H}_6-\text{N}^+(\text{Me})_3(\text{OH})^-$ groups (AF-SZN). The peak at 2 ppm in SZN is commonly assigned to terminal silanol groups.⁵ After the functionalization, it disappeared while new peaks at 5, 4, and 3 ppm are clearly seen. They can be assigned to three types of protons in $-\text{C}_3\text{H}_6-\text{N}^+(\text{Me})_3(\text{OH})^-$ groups. The lack of the original silanol peak at 2 ppm indicates that most of the silanol groups in the SZN sample probably reacted with $(\text{OEt})_3\text{-Si-C}_3\text{H}_6-\text{N}^+(\text{Me})_3(\text{OH})^-$.

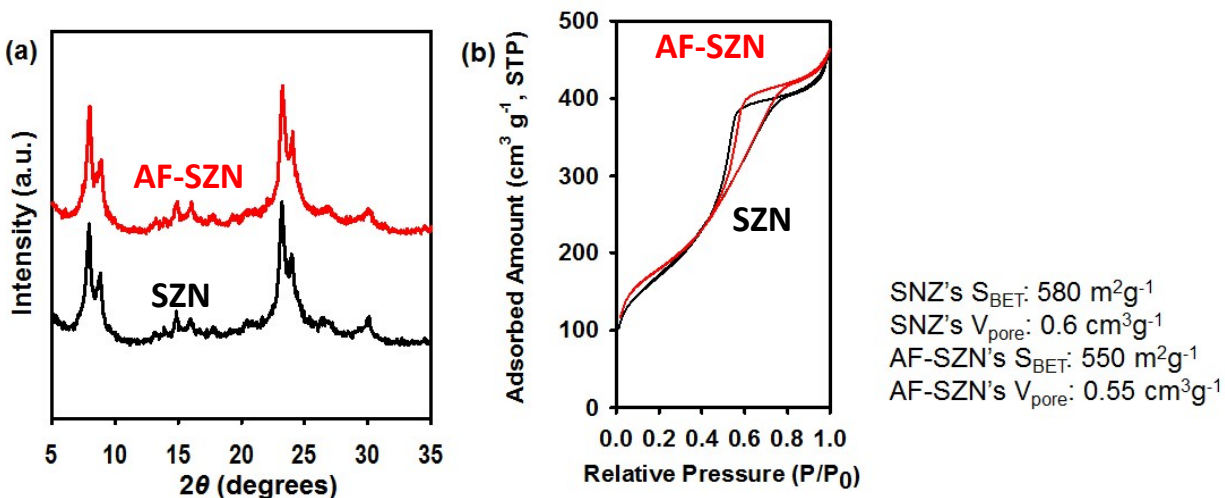


Fig. S2 XRD patterns and N_2 isotherms of SZN (black) and AF-SZN (red). As these figures show, functionalization of the SZN sample with ammonium groups had no significant effects on the zeolite crystallinity or N_2 adsorption isotherm. In particular, the N_2 adsorption isotherms in (b) indicates that the ammonium-functionalized zeolite has the same microporosity and mesoporosity as those of the pristine zeolite sample. The decrease in BET surface area or pore volume after functionalization is not significant, as confirmed by the N_2 isotherm. This means that the functionalization was achieved at a low surface density, so that ammonium groups do not block the pores markedly. See ref. 6 in ESI for the interpretation of N_2 adsorption isotherms of the MFI zeolite nanosponge.

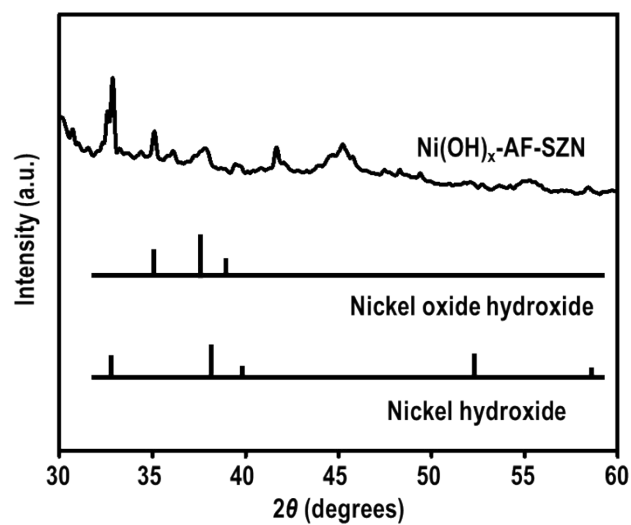


Fig. S3 XRD patterns of AF-SZN sample that was infiltrated with $\text{Ni(NO}_3)_2$ solution and dried at 100°C for 12 h. Standard JCPDS diffraction patterns for nickel oxide hydroxide [PDF card No. 000130229] and nickel hydroxide [PDF card No. 010768988] are shown for reference.



Fig. S4 Colours of SZN and AF-SZN in the phenolphthalein solution. AF-SZN exhibited a purple colour while the SZN did not.

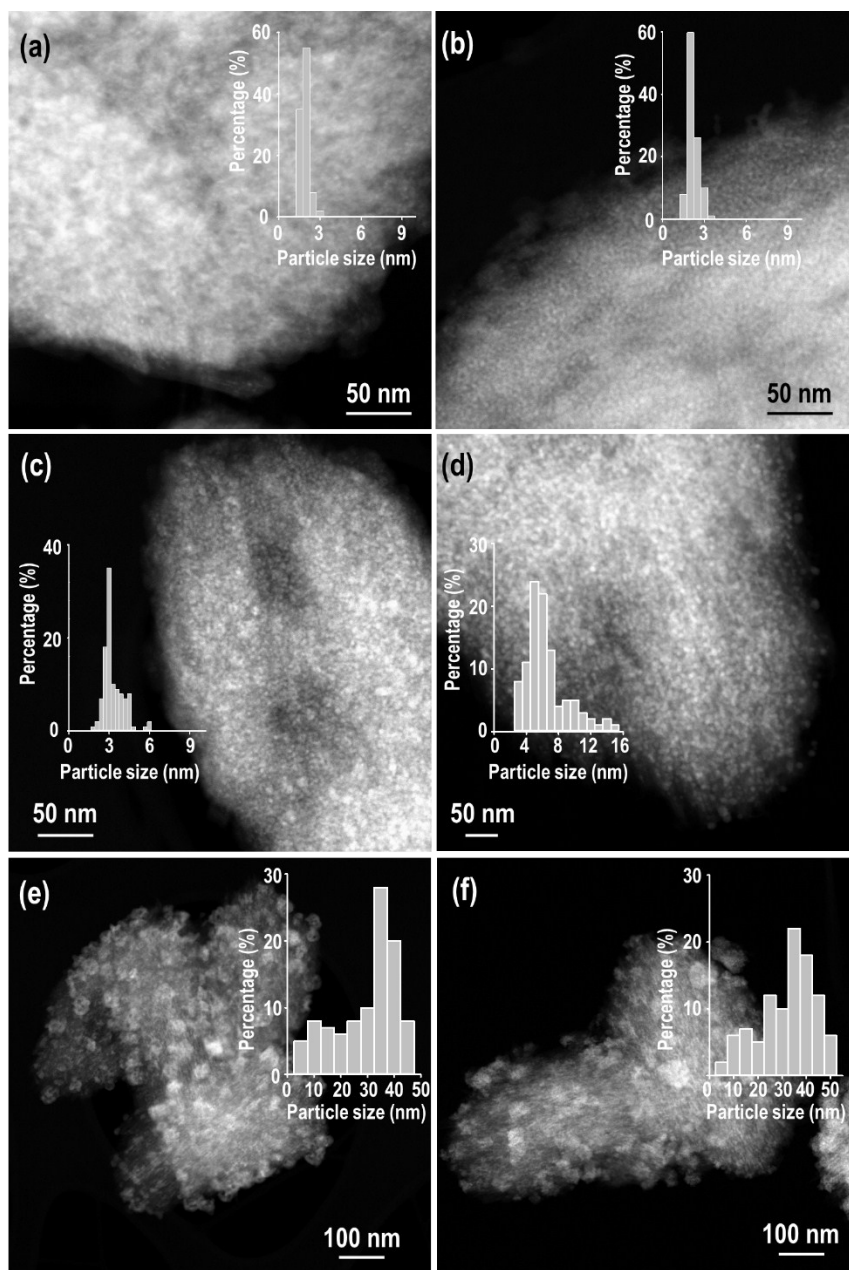


Fig. S5 STEM images of 15 wt% (a), 20 wt% (b), 25 wt% (c) and 30 wt% (d) of Ni nanoparticles supported on AF-SZN samples. For comparison, STEM images of 20 wt% (d) and 25 wt% (e) of Ni nanoparticles supported on SZN sample are displayed. The particle size distributions of Ni nanoparticles were derived from the TEM images manually and are displayed as the inset of the images. As these TEM images show, there is a dramatic decrease in Ni-particle diameters in the zeolite due to ammonium functionalization. For example, the ammonium-functionalized zeolite exhibits mostly 3.5 nm Ni particles even at 25 wt% Ni loading. On the other hand, in the case of unfunctionalized zeolite, the same Ni loading resulted in particles around 35 nm in diameter.

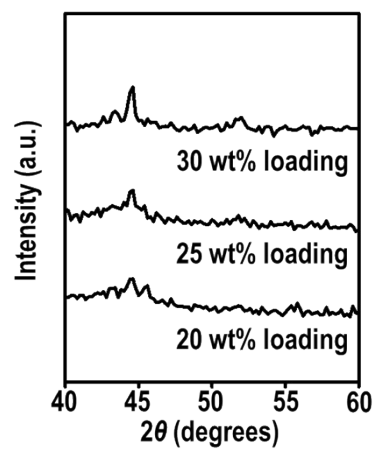


Fig. S6 XRD patterns of AF-SZN samples supporting 20 wt%, 25 wt% and 30 wt% Ni nanoparticles.

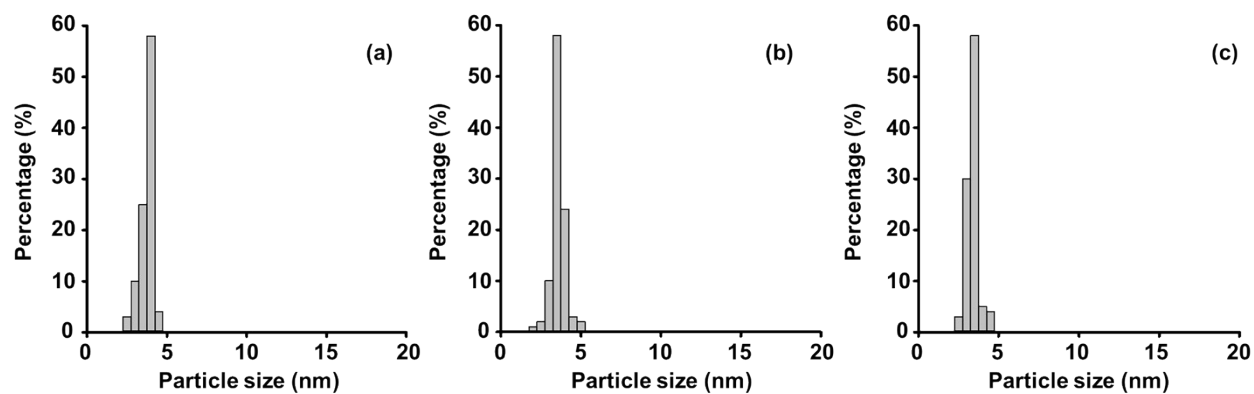


Fig. S7 The particle size distributions of Cu nanoparticles that were supported AF-SZN (a), AF-MCM-48 (b) and AF- γ -Al₂O₃ (c) samples.

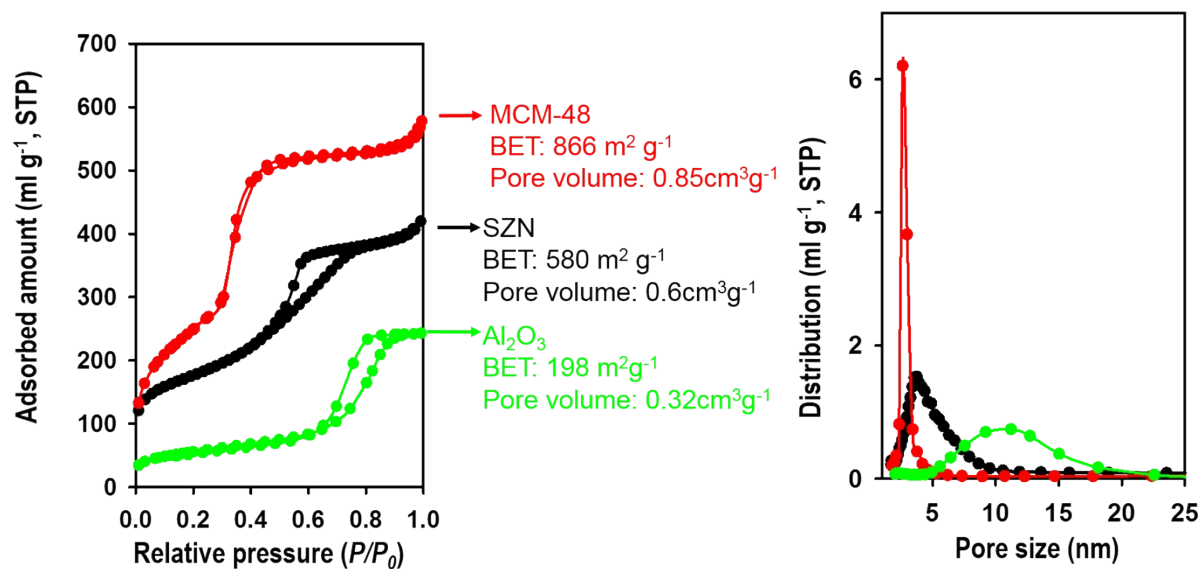


Fig. S8 N₂ adsorption-desorption isotherms and mesopore size distribution of MCM-48, SZN, and γ -Al₂O₃.

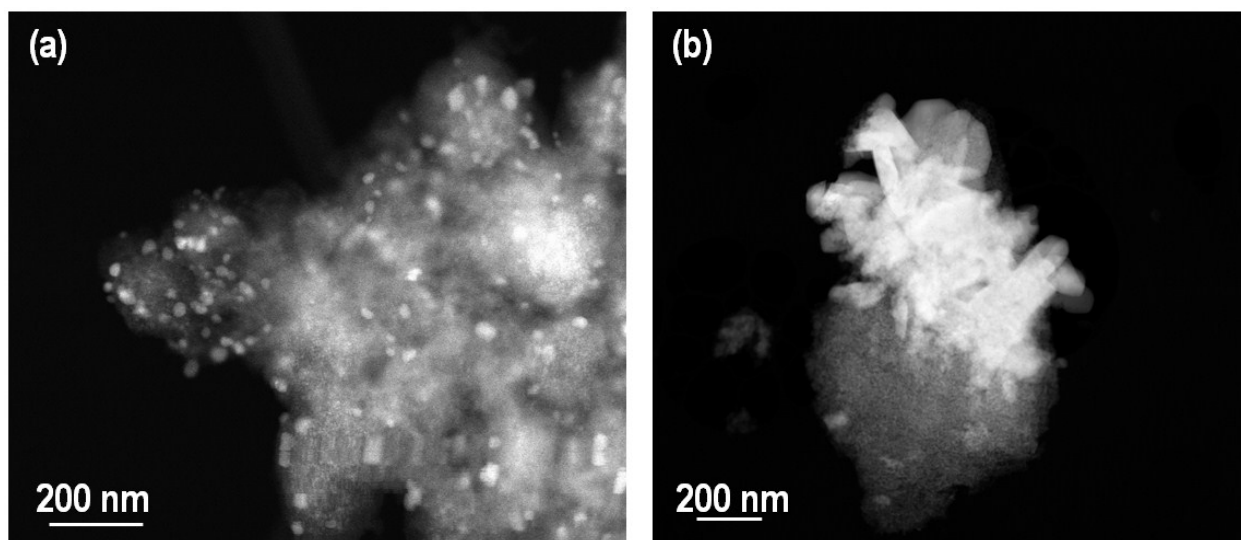


Fig. S9 STEM images of Cu supported MCM-48 and γ - Al_2O_3 samples.

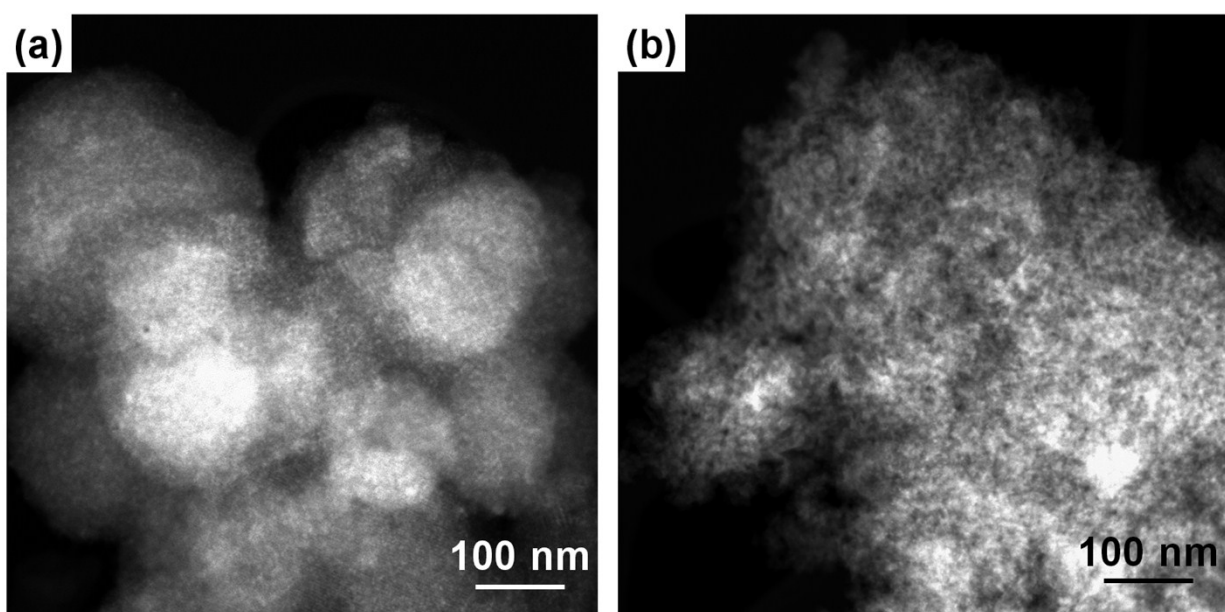


Fig. S10 STEM images of 15 wt% Ni supported AF-MCM-48 and AF- γ - Al_2O_3 samples.

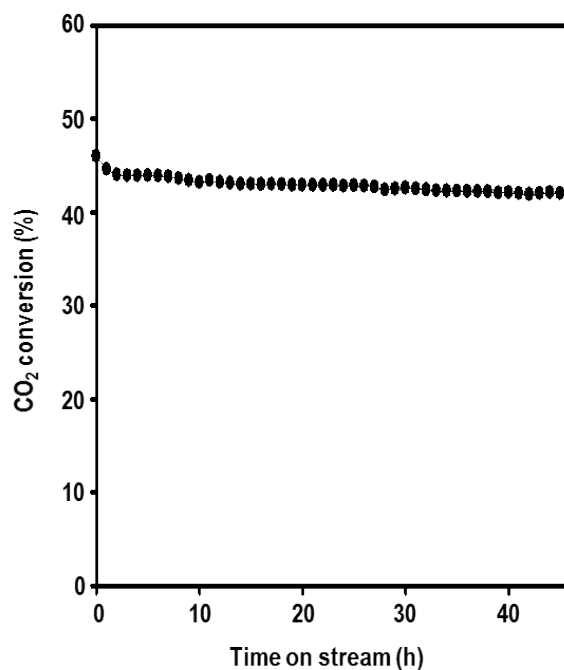


Fig. S11 CO₂ conversion over 15-Ni-AF-SZN plotted as a function of time on stream at 300 °C.

Reference.

1. K. K. Sharma and T. Asefa, *Angew. Chem. Int. Ed.*, 2007, **46**, 2879-2882.
2. R. Geyer, J. Hunold, M. Keck, P. Kraak, A. Pachulski and R. Schödel, *Chem. Ing. Tech.*, 2012, **84**, 160-164.
3. C. H. Bartholomew and R. B. Pannell, *J. Catal.*, 1980, **65**, 390-401.
4. D. G. Blackmond and E. I. Ko, *J. Catal.*, 1985, **94**, 345-352.
5. G. Buntkowsky, H. Breitzke, A. Adamczyk, F. Roelofs, T. Emmler, E. Gedat, B. Grünberg, Y. Xu, H-H. Limbach, I. Shenderovich, A. Vyalikh and G. Findenegg, *Phys. Chem. Chem. Phys.*, 2007, **9**, 4843-4853.
6. C. Jo, K. Cho, J. Kim and R. Ryoo, *Chem. Commun.*, 2014, **50**, 4175-4177.